Rapid increase of surface water pCO_2 revealed by settling particulate organic matter carbon isotope time series during 2001–2009 in Sagami Bay, Japan

Yoshihisa Mino[1], Chiho Sukigara[2], Atsushi Watanabe[3], Akihiko Morimoto[4], Kaori Uchiyama-Matsumoto[2,5], Masahide Wakita[6], and Takashi Ishimaru[2]

[1]Institute for Space-Earth Environment Research, Nagoya University, Nagoya, Japan

[2]Tokyo University of Marine Science and Technology, Tokyo, Japan

[3]The Ocean Policy Research Institute, the Sasakawa Peace Foundation, Tokyo, Japan

[4]Ehime University, Matsuyama, Japan

[5]Fukushima Cell Factory Co., Ltd., Fukushima, Japan (current affiliation)

[6]Mutsu Institute for Oceanography, Japan Agency for Marine-Earth Science and Technology, Mutsu, Japan

Corresponding author: Yoshihisa Mino (kuro@hyarc.nagoya-u.ac.jp)

Abstract

Little is known about the rate of increase of coastal seawater pCO_2 (pCO_2^{sea}), despite its necessity for assessing future oceanic CO_2 uptake capacity. We examined temporal changes in pCO_2^{sea} in central Sagami Bay during 2001–2009. Weekly pCO_2^{sea} was reconstructed using time series of particulate organic carbon isotope delta (POC-$\delta^{13}C$) of settling particles at 150 m from moored sediment trap experiments. For pCO_2^{sea} estimation, an empirical relationship between suspended POC-$\delta^{13}C$ and aqueous CO_2 concentration from repeat ship-observations in 2007–2008 was applied to the trapped POC-$\delta^{13}C$. Air-sea CO_2 flux was calculated using the air-sea pCO_2 difference with gas

transfer velocity. Estimated Bay pCO_2^{sea} varied by 190 µatm (mean 294 µatm) and was mostly below atmospheric pCO_2 (pCO_2^{air}). The mean oceanic CO_2 uptake was 82 mg m^{-2} d^{-1}, suggesting that Sagami Bay is an efficient sink for atmospheric CO_2. Meanwhile, carbon sequestration to the mesopelagic layer by particulate carbon export accounted for 60%–75% of the CO_2 uptake, with the rest likely removed horizontally via surface water exchange. The pCO_2^{sea} showed an increasing trend of +3.9 µatm y^{-1}, approximately twice that of pCO_2^{air}, and the two converged. Concurrently, a decreasing trend in POC export flux and an increasing trend in nitrogen isotope delta of trapped particles were found. Particularly, a large summer pCO_2^{sea} increasing rate (+4.9 µatm y^{-1}) was observed accompanied by POC concentration decreasing, which resulted in a decrease in CO_2 uptake over time. Long-term summer nutrient depletion and reduced primary production may increase pCO_2^{sea} in the Bay.

Keywords: coastal CO_2 uptake, pCO_2 increasing rate, Sagami Bay, particulate organic carbon export, stable carbon isotope ratio, moored sediment trap experiments

1 Introduction

Since 1850, the ocean has taken up 26% of total anthropogenic CO_2 (Friedlingstein et al., 2022), resulting in surface water pCO_2 (pCO_2^{sea}) increase and acidification over the past three decades. An analysis including millions of pCO_2^{sea} observations over a 37 year period from 1970 to 2007 (Takahashi et al. 2009) shows that contemporary oceanic water uptakes atmospheric CO_2 at 1.4 to 1.6 PgC y^{-1}, and that pCO_2^{sea} has increased at a mean rate of +1.5 µatm y^{-1}, which is comparable to that of atmospheric pCO_2 (pCO_2^{air}), suggesting that air-sea CO_2 exchange is the primary control on surface water CO_2

regulation in oceanic areas. This rate provides a basis for predicting the future CO_2 uptake capacity of the ocean that defines pCO_2^{air} levels, but it does not account for coastal CO_2 exchange with much larger variations in both spatial and temporal scales than the open ocean.

Coastal waters receive large inputs of land-driven materials that undergo active biological and chemical transformations there, consequently exchanging carbon with a variety of other pools including the atmosphere, biota, sediments, and open-ocean waters. There are limited nearshore locations where pCO_2^{sea} data are available with the high temporal resolution necessary to determine whether it is a source or sink of CO_2, and this imposes an uncertainty on the role of global oceans in atmospheric CO_2 exchange. Nevertheless, Chen et al. (2013) aggregated data from around the world and found that the global release of CO_2 from estuaries was 0.1 PgC y^{-1} and that the continental shelves absorb 0.4 PgC y^{-1}. This suggested that their combined 0.3 PgC y^{-1} absorption is equivalent to approximately 20% of the oceanic water CO_2 uptake while coastal waters represent only 7% of the surface area of oceans. Roobaert et al. (2019), using updated high-resolution (0.25°) monthly climatology data for pCO_2^{sea}, showed that the annual CO_2 uptake in coastal regions (excluding estuaries and inland water bodies) was 0.20 PgC y^{-1}, explaining approximately 12% of total oceanic CO_2 uptake. Although there were uncertainties in CO_2 exchange due to large areas that remain under sampled for pCO_2^{sea}, these results indicate a more efficient CO_2 uptake in the coastal areas than in the open ocean areas.

In addition, recent studies (Kubo et al. 2017; Tokoro et al. 2021) with dense shipboard observation data sets revealed annual-scale CO_2 unsaturation in Japan's urbanized inner bays where sewage treatment reduces the organic carbon loading, and Kubo et al. (2017)

predicted that by 2050, when urbanized coastal areas have expanded, CO_2 release by global estuaries will be less than 1/5 of current levels, resulting in increased total coastal CO_2 absorption. Thus, for future prediction of coastal CO_2 absorption, it is necessary to quantitatively assess the CO_2 exchange distribution over the entire area (including estuaries and inner bays) and to examine the long-term trend of changes in each area. In other words, further expanding pCO_2^{sea} monitoring to various coastal areas is required.

Moreover, in order to assess the sustainability of the large coastal CO_2 uptake, it is first essential to understand the mechanisms supporting its efficient carbon sequestration capacity. Although it is generally attributed to active biological activity in coastal environments (Chen and Borges 2009), there is insufficient quantitative knowledge on the fate of CO_2 absorbed: is the photosynthetically fixed organic carbon exported from the surface layer, or does it remain in the surface water or is it horizontally transported to the open ocean? Muller-Karger et al. (2005) concluded that more than 40% of the ocean carbon sequestration via the biological carbon pump (in which POC sinks) to depths below the permanent thermocline may occur along continental margins where the seafloor is shallower than 2,000 m and accounts for 13.4% of the total oceanic area. It should be noted, however, that their results were based on first-order estimates of POC flux calculated using satellite based net primary production with a single empirical model of POC remineralization in the water column in both continental margin and open ocean. This is because it is very difficult to deduce POC flux distributions from a few measurements (which are conventionally obtained by sediment trap experiment), especially at continental margins. Given the inhomogeneity of the coastal environment, the uncertainty in POC flux due to its variable attenuation in water would be extremely large. Ultimately, there are few measurement-based studies in coastal area, in which the

relationship between local CO_2 exchange and POC transport to the ocean interior can be examined.

Marine-origin particulate organic carbon isotope delta (POC-$\delta^{13}C$) is known to record the availability of dissolved CO_2 ($[CO_{2aq}]$) when organic matter is produced (O'Leary, 1981). This is due to the apparent magnitude of the ^{13}C fractionation effect (ε_p: $\delta^{13}C$ difference between the CO_2 taken up and the organic carbon formed photosynthetically) by ribulose-1,5-bisphosphate carboxylase/oxygenase (RUBISCO), which is regulated by the balance between CO_2 supply and demand (Farquhar et al. 1982). Strictly speaking, algal growth rates and cell size, which affect CO_2 demand and diffusive supply, respectively, also could constrain the ε_p (Laws et al. 1995; Popp et al. 1998), and if carbon-fixing enzymes other than RUBISCO, or active uptake of bicarbonate (with a $\delta^{13}C$ distinct from CO_2) are involved as part of the carbon concentrating mechanisms (CCM) (Raven 1997; Burkhardt et al. 2001), they may have a significant effect on ε_p (Keller and Morel 1999; Laws et al. 2002). However, the relationship between POC-$\delta^{13}C$, ε_p, and $[CO_{2aq}]$ has been recognized with a certain robustness as it applies to sedimentary POC-$\delta^{13}C$ to reconstruct paleoenvironmental CO_2 (e.g., Rau et al. 1991a; Jasper and Hayes 1990; Bentaleb and Fontugne 1998).

A moored sediment trap (MST) experiment was conducted from 2001 to 2009 at a depth of approximately 150 m at station S3 in the central part of Sagami Bay (Fig. 1; seafloor depth: ~1,500 m) where monthly hydrographical observations were made by the Tokyo University of Marine Science and Technology (TUMSAT) at that time (e.g., Hashimoto et al. 2005; Hashihama et al. 2008; Mitbavkar et al. 2009). This shallow trap experiment was conducted as part of the projects "Profiling Ocean Primary Productivity Study (POPPS)" and "POPPS-2," which aimed to develop a new autonomous, underwater

profiling buoy system and to evaluate the biological pump efficiency of Sagami Bay using the time series observations from this system combined with satellite observations (e.g., Saino 2007; Fujiki et al. 2008). The repetitive MST deployments over the nine years, despite some challenges, provided a mostly continuous time series of trapped POC-$\delta^{13}C$ and POC fluxes, which was well suited for reconstructing the surface pCO_2^{sea} in the deep bay and examining long-term changes in CO_2 exchange and POC export. Here, we aim to (1) examine a method for estimating [CO_{2aq}] using trapped particle POC-$\delta^{13}C$ in Sagami Bay to reconstruct time series of surface pCO_2^{sea} during the MST experiment, (2) examine the seasonal change and long-term trends of surface pCO_2^{sea}, and (3) examine the quantitative relationship between CO_2 and POC fluxes.

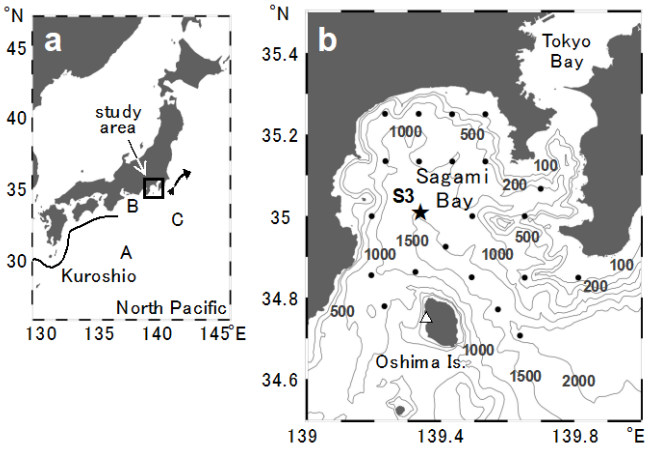

Fig. 1 (a) Location of the study area, (b) an enlarged view of the study site in Sagami Bay showing the 100, 200, 500, 1000, 1500, 2000 m isobaths. The star indicates the location of the sediment trap mooring S3 whereas the dot indicates the sampling station in the Bay. The open triangle on Oshima Island indicates the Japan Meteorological Agency weather station. In panel (a) three typical paths of the Kuroshio current are shown: A. typical large meander, B. nearshore nonlarge meander, and C. offshore nonlarge meander.

2 Materials and Methods

2.1 Moored sediment trap (MST) experiment

The MST deployments were conducted 18 times between January 2001 and July 2009, in which a cylindrical trap (610 mm length/200 mm width) fixed to a cylindrical frame (SMD26S-6000, Nichiyu Giken Kogyo, NiGK, Co. Ltd., Japan) was deployed at depths of approximately 150 and 600 m at station S3 (35.33°N, 139.33°E; Fig. 1) in central

Sagami Bay from the training vessel (T/V) Seiyo-maru belonging to TUMSAT to examine fluxes and chemical properties of settling particles. Before deployment, the collection cup was filled with seawater-based 10% buffered formalin as a preservative. The sampling interval was set to 7 days. Following trap recovery, particle samples were subsampled for microscopic observations and the rest was stored in a refrigerator until further analysis on shore. For isotopic analysis a quarter of the sample was filtered with Nucleopore polycarbonate filters (Millipore, USA) with a pore size of 0.4 μm and washed with pure water. Particles on the filters were dried at 60 °C for 36 h, weighed to calculate total mass flux, followed by grinding to obtain a homogeneous sample for subsequent chemical analysis.

2.2 Hydrographical observation and sample collections

Samples for POC-$\delta^{13}C$ of suspended particles in the Bay were collected during eight cruises (KT-07-10, May 2007; KT-07-17, July 2007; KT-07-30, November 2007; KT-08-01, February 2008; KT-08-05, April 2008; KT-08-15, July 2008; KT-08-24, September 2008; and KT-08-29, November 2008) on board the research vessel (R/V) Tansei-maru, belonging to the Japan Agency for Marine-Earth Science and Technology (JAMSTEC). Approximately 20 L of surface water was collected with a bucket at each sampling station shown in Fig. 1 (however, the number of stations varied among cruises, Online Resource 2) and filtered through pre-combusted GF/F filters (Whatman, USA). The filters were kept frozen until analysis on shore. During three cruises, KT-08-15, KT-08-24, and KT-08-29, we conducted short-term, 2 to 4 d surface-tethered drifting sediment trap (DST) experiments (Knauer et al. 1979) to collect settling particles at shallower depths than the upper MST depth. Cylindrical traps (620 mm length, 75 mm width) were filled with high-

salinity filtrated seawater (S=39, adjusted by addition of NaCl) and deployed on a drifter array in three layers between 40 and 140 m. Particles that had settled to the bottom of the traps were collected on pre-combusted GF/F filters and then frozen immediately after swimmers (i.e. mesozooplankton that entered actively sediment-trap collection bottles) on the filters were removed with tweezers. Direct underway pCO_2 measurements were conducted during three cruises in 2007 (May, July, and November), following the method used in Kayanne et al. (2005). The analyzer was calibrated using CO_2 standard gases (0 and 501 ppm) regularly during the cruises. On the five subsequent cruises in 2008, surface water samples for dissolved inorganic carbon (DIC) concentration and total alkalinity (TA) measurements were collected to estimate pCO_2^{sea}. Mercury chloride was added to water samples for DIC and TA to prevent biological activity.

2.3 Chemical analyses

Finely powdered MST samples as well as DST and suspended particles collected onto GF/F filters were exposed overnight to hydrochloric acid fumes to remove calcium carbonate ($CaCO_3$), dried in vacuum, and then pelletized with a tin disk. The POC and particulate nitrogen (PN) concentrations, and their isotope delta (POC-$\delta^{13}C$ and PN-$\delta^{15}N$, respectively) in the pellets were measured with an elemental analyzer coupled to a continuous flow isotope-ratio mass spectrometer (EA1110-DELTAplus, Thermo Fisher Scientific, USA). The precision for PN and POC mass fractions analysis was better than 3% and 5%, respectively. The precision of $\delta^{13}C$ and $\delta^{15}N$ measurements was better than 0.15‰ and 0.2‰, respectively, estimated from repeated measurements of laboratory standards (Amino Standard, SI Science, Japan) along with the samples.

The samples for DIC and TA were analyzed in the laboratory using a flow-through

analyzer (Watanabe et al. 2004). DIC and TA were measured to accuracies within 2–3 μmol kg^{-1}, based on measurements of certified reference materials from the Scripps Institution of Oceanography (distributed by Prof. Andrew Dickson). The calculated pCO_2 had an accuracy and precision of ~10 μatm from TA-DIC evaluated using the method described by Grasshoff et al. (1999, Chapter 8). The direct underway pCO_2 measurement had an accuracy of ~5 μatm and precision with a similar range or better. [CO_{2aq}] was calculated from measured pCO_2 and the solubility equilibrium constant of CO_2 in seawater (Weiss, 1974), which is a function of salinity and water temperature.

2.4 Other data

Sea surface temperature (SST) at station S3 from January 2001 to July 2002 was obtained from the mean of measurements taken at 0–5 m depths by Conductivity, Temperature, and Depth (CTD) profiler with rosette system (ICTD, Falmouth Scientific Inc., USA) during the monthly Seiyo-maru observations, and from then until July 2009 from the new generation sea surface temperature (NGSST) product provided by Tohoku University, Japan, by averaging over the area of 34.92°N–35.08°N, 139.25°E–139.42°E (approximately 18 × 15.5 km) centered on S3. Sea surface salinity (SSS) for the entire duration of trap deployments was obtained from the CTD measurement during monthly observations described above. Daily average wind speed data were provided by the Oshima weather station, Japan Meteorological Agency (JMA), located in the southern part of Sagami Bay (34.78°N, 139.36°E, elevation 74 m; Fig. 1). Daily mean atmospheric pCO_2 data from the inland pCO_2 station at Kisai, Saitama Prefecture (36.08°N, 139.55°E) were provided by The World Data Centre for Greenhouse Gases.

2.5 Calculation of air-sea CO_2 flux

The air-sea CO_2 flux was calculated as follows:

$$CO_2 \text{ flux} = k_{CO2}\, K_0\, (pCO_2^{sea} - pCO_2^{air}) = k_{CO2}\, K_0\, \Delta pCO_2 \qquad \text{Eq. 1}$$

where k_{CO2} is the gas exchange coefficient calculated following Wanninkhof (2014). The pCO_2^{air} indicates atmospheric pCO_2, and ΔpCO_2 is the difference between pCO_2^{sea} and pCO_2^{air}. Note that negative values of the flux indicate oceanic CO_2 uptake. The time scale for each parameter and thereby the flux is weekly. The weekly pCO_2^{air} was derived from water vapor-corrected daily mean data. The weekly wind speed at 10 m above the sea surface, U_{10}, which is required to calculate k_{CO2}, was obtained from daily wind speed data from the Oshima weather station, corrected for altitude and further corrected using an empirical relationship derived from a comparison with actual sea winds measured at S3 during the cruise. Estimated weekly U_{10} during the whole sediment trap experiment period ranged from 3.1–10.4 m s^{-1}.

2.6 Calculation of deseasonalized monthly means

In this study, following Takahashi et al. (2006) and Wakita et al. (2021), we removed potential seasonal bias of sampling from the observed and estimated values and examined long-term changes in physical and chemical parameters. For example, the deseasonalized monthly mean of seawater pCO_2, $pCO_{2\ \text{deseasonalized}}$, was calculated as follows:

$$pCO_{2\ \text{deseasonalized}} = pCO_{2\ \text{est}}^{\ \text{month}} - pCO_{2\ \text{mean}}^{\ \text{month}} + pCO_{2\ \text{mean}}^{\ \text{annual}} \qquad \text{Eq. 2}$$

where $pCO_{2\ \text{est}}^{\ \text{month}}$ is the mean of estimated pCO_2 for each month, and $pCO_{2\ \text{mean}}^{\ \text{month}}$ and $pCO_{2\ \text{mean}}^{\ \text{annual}}$ are the monthly and annual mean values for the entire period of data acquisition, respectively. The rate of change of these deseasonalized monthly means time series was calculated using a linear least-squares method and was considered statistically

significant at $p < 0.05$. The error value for the rate is the standard error of the linear regression slope.

3 Results

3.1 Variations in POC export and POC-$\delta^{13}C$

The POC flux ranged from 3.9–513 mg m^{-2} d^{-1} with a mean of 53 ± 46 mg m^{-2} d^{-1} for the duration of all trap deployments, with a mean of 53 ± 44 mg m^{-2} d^{-1} for the period 2001–2008 (Fig. 2a, Table 1). Although sporadic spike fluxes occurred, exceptions included continuous high fluxes > 100 mg m^{-2} d^{-1} in April–May and September–December 2006. Excluding high fluxes in the top 5% (> 120 mg m^{-2} d^{-1}), seasonal variation occurred with higher and lower fluxes in summer (June to August) and winter (December–February), respectively. The POC-$\delta^{13}C$ of trapped particles varied from −28.0‰ to −17.8‰ with a mean of −21.9 ± 1.5‰ (Fig. 2b). Most of the high POC-$\delta^{13}C$ values (> −20‰) including the maximum were found in 2006, particularly during the high flux event from September to December. Shipboard observations conducted on 13 October 2006 revealed that large (> 50 μm) diatoms *Pseudo-nitzschia* spp. were abundant in the surface water of Sagami Bay at trap location S3. On the same day, the Bureau of Environment, Tokyo Metropolitan Government (https://www.kankyo.metro.tokyo.lg.jp/water/tokyo_bay/red_tide/download.html, in Japanese) determined that these diatoms were the cause of the red tide in the inner part of Tokyo Bay. In addition, surface chlorophyll (Chl) *a* spreading from within Tokyo Bay to central Sagami Bay was observed in satellite ocean color images (MODIS, Online Resource 1) during the period 16–23 October. These findings suggest that particulate organic matter with high $\delta^{13}C$ (−19‰ to −16‰: Sukigara and Saino 2005, Sukigara et al. 2022) of planktonic origin

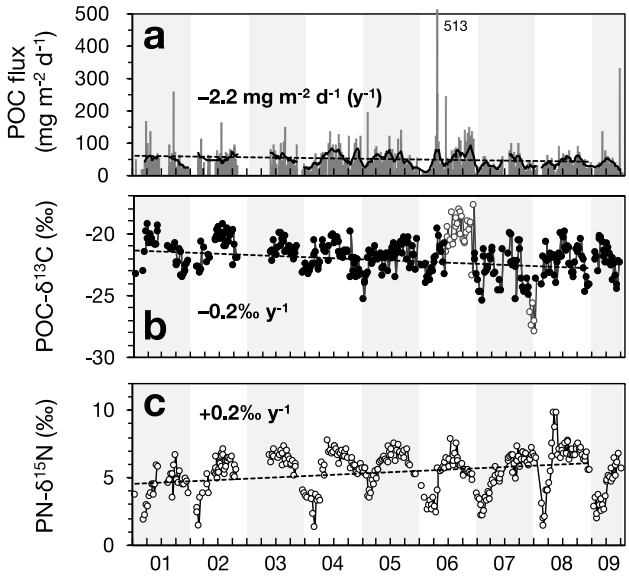

Fig. 2 Time series data of (a) particulate organic carbon (POC) flux (bar), (b), particulate organic carbon isotope delta (POC-δ^{13}C, closed circle) and (c) particulate nitrogen isotope delta (PN-δ^{15}N, open circle) of trapped particles at 150 m in central Sagami Bay during 2001–2009. Thick line in panel a indicates 6-week moving average of POC flux after excluding the top 5% high fluxes. Dashed lines in panels indicate statistically significant regressions of deseasonalized monthly means ($p < 0.05$). Note that these regressions were obtained after excluding all data from 2006 and the end of 2007, when extreme values of POC-δ^{13}C were found (see text).

within Tokyo Bay probably entered the trap in 2006. In contrast, the very low POC-δ^{13}C data (< −27‰, including the lowest value recorded) from December 2007 to early January 2008 appeared at the same time as a very strong cold wave under a strong to super La Niña event (with the bi-monthly NCEP–NCAR Multivariate ENSO Index of < −1.5); the shipboard observation immediately afterwards (18 January 2008) reported that the surface layer at S3 was mixed deeply (i.e., beyond 120 m). This deep mixing may have contributed to the formation of particles with low POC-δ^{13}C. Overall, POC-δ^{13}C showed a seasonal cycle of low and high in winter and summer, respectively, with a mean change of approximately 3.5‰. Excluding the extreme values of POC-δ^{13}C in June–December 2006 and December 2007, there was a significant declining trend (−0.2 ± 0.0‰ y^{-1}, $p < 0.001$) for the deseasonalized monthly mean of POC-δ^{13}C over the period 2001–2008, whereas there was no significant trend for the POC flux. However, when data from the first half of 2006, including outlier POC flux with high δ^{13}C, were also excluded, a significant decreasing trend ($p = 0.00654$) of −2.2 ± 0.8 mg m^{-2} d^{-1} (y^{-1}) was apparent in the POC flux (Table 2).

3.2 CO_2-dependence of suspended POC-$\delta^{13}C$ and its application to trapped POC-$\delta^{13}C$

Suspended POC-$\delta^{13}C$ in surface waters of the Bay sampled during 2007 and 2008 varied from −25.6‰ to −15.4‰ (Fig. 3). No clear spatial variation was found during the period when there was a deeper mixed layer depth (MLD) where the water temperature changed by 0.5 °C from the SST (e.g., 60 m at S3 in November 2007). However, during the period with stratified water structures with shallower MLDs of 7–10 m in July in 2007 and 2008, the POC-$\delta^{13}C$ values were higher along the northern coast of the Bay and lower in the southern part facing the open ocean (Fig. 4e–h). The POC-$\delta^{13}C$ also varied seasonally with higher and lower values found in summer and winter, respectively (Online Resource 2). Spatio-temporal variation in POC-$\delta^{13}C$ of 10‰ was strongly inversely correlated with changes in surface water aqueous CO_2 concentration, [CO_{2aq}] ($r = 0.84$, $p < 0.001$, Fig. 3). This relationship is constrained by ^{13}C fractionation associated with photosynthetic carbon fixation in the CO_2 supply and demand model (Farquhar et al. 1982): larger ε_p under higher [CO_{2aq}] condition results in POC production with lower $\delta^{13}C$, and vice versa. POC-$\delta^{13}C$ vs. [CO_{2aq}] relationships have been used to reconstruct the CO_{2aq} environment at the time when organic matter was formed, and the slope of our relationship of −1.04‰ μM^{-1} was within the previously reported range (−1.5‰ μM^{-1} to −0.6‰ μM^{-1}, Rau 1994; Fischer et al. 1998, Bentaleb et al. 1998). The magnitude of temporal change in suspended POC-$\delta^{13}C$ at S3 was ~5‰, which followed well the POC-$\delta^{13}C$ vs. [CO_{2aq}] regression derived from the dataset throughout Sagami Bay. This relationship was applied to POC-$\delta^{13}C$ data for trapped particles obtained during the same period as the cruise observations in 2007–2008 to estimate [CO_{2aq}] and the corresponding pCO_2^{sea} when the trapped particles were formed. Those trapped POC-$\delta^{13}C$-based estimates were in good agreement

with the actual pCO_2^{sea} measurements at S3 during the observations (RMSE = 28 μatm, n = 8; Online Resource 2).

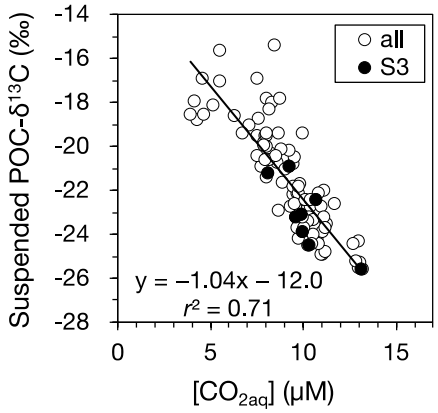

Fig. 3 Relationship between suspended POC-$\delta^{13}C$ and aqueous CO_2 concentration ($[CO_{2aq}]$) in surface waters collected during 2007 to 2008 in Sagami Bay. Closed and open circles indicate data from station S3 and others.

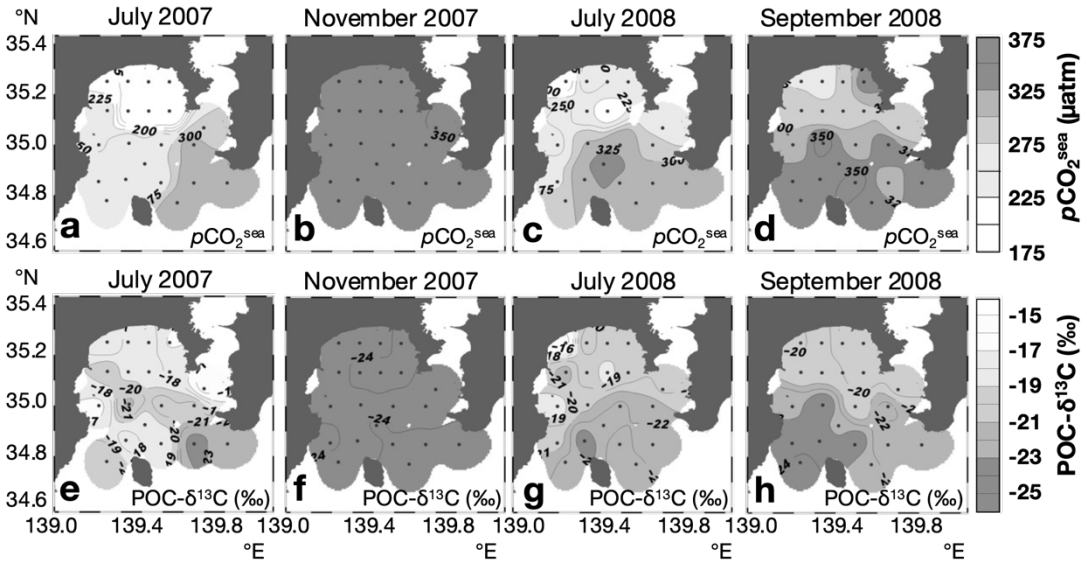

Fig. 4 Distribution of surface water pCO_2 (pCO_2^{sea}) and suspended POC-$\delta^{13}C$ in Sagami Bay in (a, e) July 2007, (b, f) November 2007, (c, g) July 2008, and (d, h) September 2008. Note that pCO_2^{sea} data in 2007 were obtained by underway measuring system on board while those in 2008 were calculated from both measurements of dissolved inorganic carbon and total alkalinity of surface water samples.

3.3 Temporal variation of pCO_2^{sea} and CO_2 flux

The pCO_2^{sea} estimation method using the empirical POC-$\delta^{13}C$ vs. $[CO_{2aq}]$ relationship, described in section 3-2, was applied to all trapped POC-$\delta^{13}C$ data to reconstruct surface pCO_2^{sea} in the Bay from 2001 to 2009. The CO_2 solubility K_0 used here was derived from

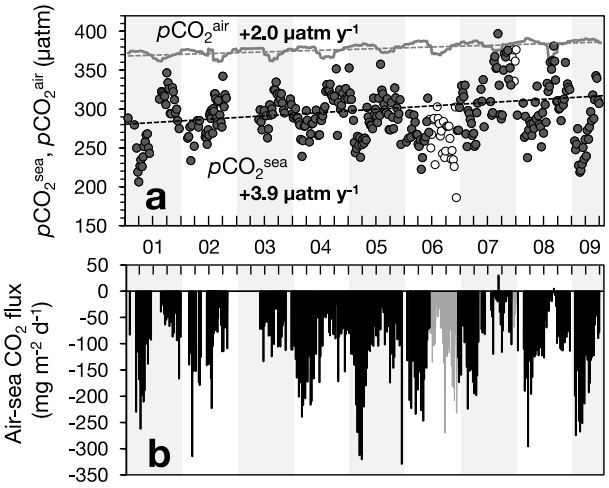

Fig. 5 Time series data of (a) pCO_2^{sea} (circle) and atmospheric pCO_2 (pCO_2^{air}, solid line), (b) air-sea CO_2 flux (bar) in the central part of Sagami Bay during 2001 to 2009. For CO_2 flux, negative values indicate oceanic CO_2 uptake. Open circles in panel (a) indicate pCO_2^{sea} calculated from "extreme POC-δ^{13}C values" (see text). CO_2 fluxes associated with these extreme δ^{13}C are presented as gray bars in panel (b). Dashed lines in panel a indicate statistically significant regressions of deseasonalized monthly means ($p < 0.05$). Note that these regressions were obtained after excluding all data from 2006 and the end of 2007, when extreme values of POC-δ^{13}C were found.

the SST and SSS at S3 for each particle collection period.

Estimated pCO_2^{sea} varied from 186 to 396 µatm (mean 292 ± 34 µatm) and showed seasonality, with lower and higher values in spring (March to May) and autumn (September to November), respectively (Fig. 5a, Table 1). During the 8.5-year period, it was consistently below the pCO_2^{air} level (361–391 µatm with a mean of 377 ± 7 µatm), with exceptions in September 2007 and September 2008. CO_2 flux varied from −266 to +25 mg m^{-2} d^{-1} with a mean of −88 ± 51 mg m^{-2} d^{-1} (in carbon equivalents; Fig. 5b). Note that given the relative error of the pCO_2^{sea} estimate of 9% and that of k_{CO2} of 20% (Wanninkhof, 2014), the propagated error of the CO_2 flux was calculated to be 29%. Higher CO_2 uptake occurred in winter and spring compared to that in other seasons (Table 1). The correlation coefficients of k_{CO2}, K_0, and air-sea pCO_2 difference ($pCO_2^{sea} - pCO_2^{air}$, hereafter ΔpCO_2) to CO_2 flux were −0.52, −0.63, and 0.79 (all with $p < 0.001$, $n = 359$), respectively. Except for the second half of 2006 and the end of 2007 when the extreme POC-δ^{13}C values (mentioned in section 3-1) were observed, the deseasonalized monthly mean of pCO_2^{sea} between 2001 and 2008 showed an increasing trend (+3.6 ± 0.7 µatm y^{-1}, $p < 0.001$) attributable to a decrease in POC-δ^{13}C. Furthermore, if the data for the first

half of 2006 were also excluded, the rate was +3.9 ± 0.7 μatm y^{-1} ($p < 0.001$, Table 2). This is well above the increase of pCO_2^{air} (+2.0 ± 0.1 μatm y^{-1}, $p < 0.001$), resulting in an upward trend of +1.9 ± 0.7 μatm y^{-1} ($p = 0.00750$) for ΔpCO_2 indicating that the two were converging. Meanwhile, no significant trend for CO_2 flux was detected.

4 Discussion

4.1 POC-$\delta^{13}C$–based pCO_2^{sea} estimation

The POC-$\delta^{13}C$ signal with an inverse linear trend with [CO_{2aq}] has been used to estimate paleoenvironmental pCO_2 from sedimentary POC-$\delta^{13}C$ records (Rau et al. 1991a; Jasper and Hayes 1990; Bentaleb and Fontugne 1998). For application of it in the Southern Ocean, where it may have contributed to glacial–interglacial changes in the control of atmospheric CO_2 (e.g. François et al., 1997), various relationships between POC-$\delta^{13}C$ and [CO_{2aq}] from this region have been reported with slopes (i.e. the sensitivity of POC-$\delta^{13}C$ to [CO_{2aq}]) of −1.1‰ μM^{-1} to −0.6‰ μM^{-1} (Rau et al. 1989, 1991b; Francois et al., 1993; Kennedy and Robertson 1995; Dehairs et al. 1997; Bentaleb et al. 1998; Lourey et al. 2004). Even steeper slopes (to −1.5‰ μM^{-1}) of the regression have been found in the Northeast Atlantic (Rau et al. 1992) and the tropical–subtropical Atlantic (Fischer et al. 1998). Notably, there was a large difference in the range and variation of [CO_{2aq}] among datasets, however, the slope is likely to be steeper in regions where biological activity is the dominant control on [CO_{2aq}] than it is in regions with temperature (solubility)-controlled [CO_{2aq}]. The regression with a slope of −1.5‰ μM^{-1} presented by Rau et al. (1992) was obtained from time-course observations during a phytoplankton bloom in the NABE (North Atlantic Bloom Experiment) site, whereas the global (open ocean) data compilation-based relationship by Rau (1994) showed a slope of −0.63‰ μM^{-1}. The slope

of our empirical regression for Sagami Bay data was −1.04‰ μM^{-1} (Fig. 3), which is in the middle of the previously reported values. This is probably due to the different features of the deep bay in a temperate region: active biological processes occur as are typical of coastal waters, meanwhile the upper layer condition of the Bay which has an annual SST cycle of that varies by 12 °C, is strongly influenced by open water (i.e., Kuroshio warm water; Hinata et al. 2003). The CO_2 dependence of POC-$\delta^{13}C$ is possibly disturbed by algal growth rates and cell size as well as the presence of CCMs (Laws et al. 1995; Popp et al. 1998; Keller and Morel 1999; Laws et al. 2002). However, the strong correlation (r^2 = 0.71) between POC-$\delta^{13}C$ and [CO_{2aq}] suggests that the compound effects of these changes were eventually minor, at least for surface water POM in Sagami Bay.

Suspended POC-$\delta^{13}C$ in the euphotic zone is assumed to primarily reflect the $\delta^{13}C$ signal of autotrophs (i.e., phytoplankton), whereas trapped POC-$\delta^{13}C$ could be influenced by heterotrophic processes (trophic transfer and microbial degradation; DeNiro and Epstein 1978; Fry, 1988; Aita et al. 2011 etc.). However, the 2–4 days surface tethered DST experiments at S3 in July and November 2008 showed POC-$\delta^{13}C$ of the settling particles at 40–140 m with −22.1±0.6‰ and −22.8±0.2‰, respectively, which were comparable to the surface water suspended POC-$\delta^{13}C$ (with a difference by ~0.4‰) although POC-$\delta^{13}C$ of DST particles in September (−21.5 ± 0.1‰) deviated positively from suspended POC-$\delta^{13}C$ by 1.1‰ (Online Resource 3). Moreover, the mean difference in POC-$\delta^{13}C$ from the MST particles collected near the DST deployment period was −0.2 ± 1.0‰. For a thorough comparison between MST, DST, and suspended particles, the differences in sampling period (MST: 7 days, DST: 2–4 days) as well as the time scale in which suspended POC-$\delta^{13}C$ changes should be considered. However, overall consistency of POC-$\delta^{13}C$ among them suggested that heterotrophic $\delta^{13}C$ modification to trapped

particles was small. Even if it had occurred, particles trapped at 150 m would have had a short time to undergo microbial degradation as they sunk from the euphotic layer. In fact, the mean of the trapped particulate organic carbon-to-nitrogen (C:N) mole ratio was 8.1 ± 2.2, which is substantially lower than that of deep layer trapped particles in coastal regions: mean C:N of 9.2 at 750 m at Tokyo Bay mouth (Sukigara and Saino 2005); 8.9–13.7 at ~1300 m off Mauritania, Atlantic Ocean (Fischer et al. 2021). The increases in trapped particle C:N with depth have been revealed by multi-layer MST deployments in oceanic time series stations: e.g., BATS (31°40N, 63°10W), 7.8 ± 1.4 at 500 m and 9.7 ± 1.4 at 3,200 m (Conte et al. 2001); K2 (47°N, 160°E) 8.2 ± 2.7 at 500 m, 9.9 ± 3.8 at 4810 m (Mino et al. 2016; JAMSTEC K2S1 database, https://ebcrpa.jamstec.go.jp/k2s1/en/index.html). Given that a C:N ratio increases with the degree of degradation in which N-rich organic matter is consumed preferentially (Waples and Sloan, 1980), the trapped POM by our shallow MST at Sagami Bay was likely composed of relatively fresh material.

Thus, nearly continuous collection of trapped POC-$\delta^{13}C$ data with less heterotrophic $\delta^{13}C$ modification and a 1-week resolution is of great importance as it was used to estimate pCO_2^{sea} in the central part of the deep bay where monitoring facilities are difficult to construct. The eventual estimation accuracy of 28 μatm is much larger than the pCO_2^{sea} measuring precision of approximately 5 μatm (Roobaert et al., 2019) and cannot contribute to a global database such as SOCAT (Bakker et al, 2016). However, it is sufficient to evaluate changes in pCO_2^{sea} with a seasonal amplitude (maximum minus minimum) of ~150 μatm. Moreover, it is smaller than the increase of the deseasonalized pCO_2^{sea} over 8.5 years (i.e., +3.9 μatm y^{-1} × 8.5 years = 33.2 μatm), thus our detected increase rate of pCO_2^{sea} is substantial.

4.2 Evaluation of CO_2 uptake in Sagami Bay

Estimated surface pCO_2^{sea} in central Sagami Bay was below pCO_2^{air} for most of the observation period, with atmospheric CO_2 absorbed at a mean flux of −82.1 mg m^{-2} d^{-1} or −30.0 g m^{-2} y^{-1} (Fig. 5b). The mean CO_2 uptake flux for the entire Sagami Bay region was likely higher because the pCO_2^{sea} measurements at S3 during stratified periods (July and September) were higher than those at nearshore stations on the north side of the Bay where active biological CO_2 consumption likely occurred (Fig. 4a–d; Online Resource 2). Nevertheless, the annual CO_2 uptake flux in central Sagami Bay is still 6.1 times higher than the global mean of climatological values (based on a vast volume of measured data) of −4.9 g m^{-2} y^{-1} and 3.0 times larger than the Northern Hemisphere temperate (14°N–50°N) average of −10.1 g m^{-2} y^{-1} (Takahashi et al. 2009). Moreover, it is comparable to, or slightly lower than, the considerably large CO_2 uptake of −34 to −39 g m^{-2} y^{-1} (Kubo et al. 2017; Tokoro et al. 2021) of the adjacent Tokyo Bay. Note that the k_{CO2} scaling factors used in these flux calculations were almost the same: 0.251 for this study and Tokoro et al. (2021) and 0.26 for Takahashi et al. (2009). This adequate comparison suggests that Sagami Bay is an efficient sink for atmospheric CO_2.

The mean POC flux at 150 m, i.e., the amount of carbon exported from the surface layer to deep water, was 18.1 g m^{-2} y^{-1} (= 50 mg m^{-2} d^{-1}), corresponding to 60% of the CO_2 uptake at the sea surface. In general, shallow MST experiments raise concerns regarding particle under-trapping due to hydrodynamic effects (Buesseler et al. 2007). Honda et al. (2015) reported that POC flux into cylindrical DSTs was on average 3–4 times higher than those into conical MSTs when comparing flux data at 200 m from both DST and MST experiments conducted in time series stations of subarctic K2 and subtropical S1 in

the western North Pacific. However, the POC flux vertical attenuation derived from our multi-layer (40−140 m) DSTs flux data at S3 was consistent with the MST flux data at 150−160 m (Online Resource 3). This consistency was partly attributable to our MST having a cylindrical mouth like DSTs though its aspect ratio (*A*, length/width) of 3.05 was lower than the DST's *A* of 8.27. Under calm conditions, like when our DST experiments were conducted, surface-tethered DSTs have a comparable particle trapping efficiency to the neutrally buoyant sediment traps that are hardly affected by hydrodynamic biases (Buesseler et al. 2000). When these are considered, our MST-derived POC flux at Sagami Bay was likely close to the true flux, and far from undervalued.

Unfortunately, there were no data for particulate inorganic carbon (PIC) flux associated with $CaCO_3$ in the trapped particles. In the surface layer of S3 in central Sagami Bay, the Haptophytes-3 group (primarily coccolithophytes) was present with a minor contribution to total Chl *a* whenever the influence of Tokyo Bay water was small (Hashihama et al. 2008). Based on the particle fluxes from deep sediment traps in Sagami Bay reported by Masuzawa et al. (2003), the trapped POC:PIC flux ratio at ~1,200 m was 66:15.8. Even if this ratio was applied to our POC fluxes at a shallower depth (a poor assumption, given that organic carbon in settling is more readily degraded than $CaCO_3$), the total carbon flux would still be 22.4 g m^{-2} y^{-1}, only 75% of CO_2 uptake. Dissolved organic carbon could also be exported vertically, however, since it depends primarily on seawater sinking, i.e., downwelling (Walsh et al. 1992), we do not consider its contribution. Rather, DOC would be removed by horizontal transport. If steady state conditions hold with respect to the surface layer carbon budget, then 25%–40% of the CO_2 absorbed was probably removed by horizontal water exchange with waters from outside of the Bay.

The upper environment of Sagami Bay (~250 m) is influenced by the Kuroshio warm

water intrusion through the Oshima west and east channels, which are closely related to the Kuroshio path rather than by the inflow of Tokyo Bay water. For example, when the Kuroshio takes a typical large meander (Fig. 1a), Kuroshio warm water strongly intrudes into the Bay through the west channel and then flows out through the east channel when southward to southwestward winds dominate in winter (Hinata et al. 2003). This flow may transport surface water containing abundant absorbed CO_2 in winter out of the Bay. Moreover, if the temperature of the inflowing Kuroshio water drops as it flows into the Bay, it would lower pCO_2^{sea} by increasing gas solubility, thus absorbing atmospheric CO_2 before it flows out of the Bay. This theory should be tested in the future. Although our estimated CO_2 flux had a relative error of 29%, the results may indicate that downward POC flux in the water was smaller than the atmospheric CO_2 influx to the ocean. This suggests that CO_2 absorbed in a given coastal area is not necessarily exported as particulate carbon to the mesopelagic layer; its fate is important to consider when evaluating atmospheric CO_2 sequestration.

4.3 Seasonal changes in pCO_2^{sea} and CO_2 uptake

CO_2 uptake was approximately twice as high in winter and spring than that in summer and autumn (Table 1). This is primarily because pCO_2^{sea} was lower in winter and spring, accompanied by a higher gas exchange coefficient due to higher wind speeds in winter. The seasonal variation in pCO_2^{sea}, with minimums in March–April, maximums in August–October, and an amplitude of 190 μatm, was sinusoidal and likely followed the annual cycle of 12 °C SST fluctuations with a time lag of ~1 month (Fig. 6a). This is because, in addition to the major effect of SST that determines gas solubility, changes in DIC (depending on vertical and horizontal DIC supply and biological DIC consumption)

affect pCO_2^{sea}. Here, following Takahashi et al. (2002), we separated seasonal pCO_2^{sea} with changes in SST and DIC using the following equations:

$$pCO_2^{sea} \text{ at } T_{obs} = (pCO_2^{sea})_{mean} \exp[0.0423(T_{obs} - T_{mean})], \quad \text{Eq. 3}$$

$$pCO_2^{sea} \text{ at } T_{mean} = (pCO_2^{sea})_{obs} \exp[0.0423(T_{mean} - T_{obs})], \quad \text{Eq. 4}$$

where T is the SST and the subscripts "obs" and "mean" indicate the observed and annual mean values, respectively. A $(pCO_2^{sea})_{mean}$ of 296 μatm and T_{mean} of 20.6 °C were used. The experimentally determined temperature sensitivity factor, $\partial \ln pCO_2^{sea}/\partial T$ = 0.0423 $°C^{-1}$ (Takahashi et al. 1993), was used. Here, we used the pCO_2^{sea}, which linearly excludes the increasing trend of +3.9 ± 0.7 μatm y^{-1} described above, with respect to that on 1 January 2005. The pCO_2^{sea} in equations 3 and 4 were referred to as isochemical- and isothermal-pCO_2^{sea}, respectively (Keeling et al. 2004), and these seasonal amplitudes indicate the magnitudes of the effect of SST and DIC changes, which were calculated to be 155 and 144 μatm, respectively (Fig. 6b). The biological pCO_2^{sea} drawdown expected from a seasonal decrease of dissolved inorganic nitrogen (DIN) of 10–11 μM in surface

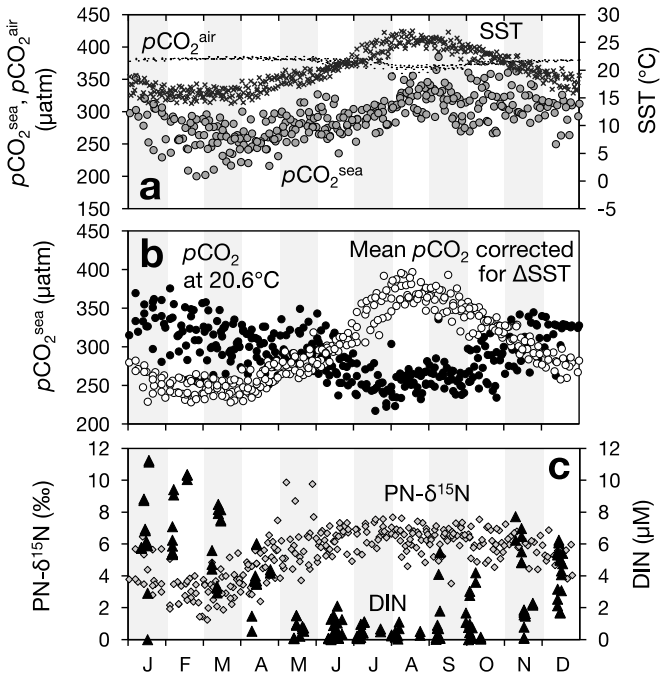

Fig. 6 Annual composite time series of (a) seawater pCO_2^{sea} (circle), atmospheric pCO_2^{air} (dot), and sea surface temperature (SST, cross), (b) pCO_2^{sea} values normalized to the mean annual temperature of 20.6° C (isothermal pCO_2^{sea}; closed circle) and the mean annual pCO_2^{sea} values corrected for temperature changes (isochemical pCO_2^{sea}; open circle), and (c) trapped PN-$\delta^{15}N$ and dissolved inorganic nitrogen (DIN) concentration in the surface waters at S3. The pCO_2^{sea} and pCO_2^{air}, SST and trapped PN-$\delta^{15}N$ were obtained during 2001 to 2009 while DIN concentrations were observed during 2001 to 2007. Note that the linearly de-trended pCO_2^{sea} values for the long-term change are presented in panel a and were used to calculate both isochemical pCO_2^{sea} and isothermal pCO_2^{sea} in panel b (see text). The PN-$\delta^{15}N$ in panel c was also de-trended.

water at S3 (Fig. 6c) with a Redfield C:N ratio of 106:15, Revelle factor of 10 (Sabine et al. 2004), and winter typical DIC of 2065 μM (measured in February 2008), was 129–142 μatm, which is in close agreement with the calculated seasonal amplitude of isothermal-pCO_2^{sea} of 144 μatm. This supports the validity of the equation.

The isochemical-pCO_2^{sea} reached a minimum of 220–230 μatm in February–March owing to increased solubility with winter cooling, and then increased to ~390 μatm until August owing to the effects of seasonal warming. In contrast, isothermal-pCO_2^{sea} had a maximum of 386 μatm in January–February owing to DIC enrichment associated with winter mixing, and then gradually decreased from March, 1 month before water temperature increases, to < 230 μatm in July when nutrients were depleted, primarily owing to biological consumption (i.e., phytoplankton CO_2 uptake). The accompanying decrease in DIN and summer depletion can also be seen as a gradual rise in trapped PN-$\delta^{15}N$ during that period (Fig. 6c), which is because the remaining nitrate $\delta^{15}N$ rises due to the ^{15}N fractionation effect associated with nitrate uptake by phytoplankton (Miyake and Wada 1967). The active organic matter production resulted in high POC export flux in spring and summer (Table 1). Subsequently, isothermal-pCO_2^{sea} increased again from October, probably due to DIC supplied by mixing. In fact, surface water DIN of more than 4 μM was found occasionally in October–November (Fig. 6c). The combined effects of these temperature and biological DIC changes determine the seasonal variation in pCO_2^{sea}. As in the temperate open ocean, the temperature effect exceeds the DIC effect (but only slightly) in Sagami Bay. However, the biological CO_2 drawdown effect in the Bay (144 μatm) is large on a global scale as effects exceeding 140 μatm are primarily found only in productive high-latitude oceans north of 40°N, and only below 50 μatm in the vast tropical and subtropical areas (Takahashi et al. 2002).

4.4 Long-term trends in pCO_2^{sea} and CO_2 uptake in Sagami Bay

Although there was no significant trend in the deseasonalized CO_2 flux in Sagami Bay, there was a significant upward trend in ΔpCO_2, the primary source of variation in CO_2 flux, of +1.9 μatm y^{-1} (i.e., pCO_2^{air} and pCO_2^{sea} converged by 1.9 μatm each year). If maintained, this is likely to lead to a decrease in CO_2 uptake in the Bay in the long term. The increase rate of pCO_2^{sea} (+3.9 μatm y^{-1}), which was approximately twice that of pCO_2^{air} (+2.0 μatm y^{-1}), is quite large compared to those in other ocean regions: the global open ocean average during 1970–2007 was +1.5 μatm y^{-1} (Takahashi et al. 2009), whereas the highest basin-scale rate was approximately +2.1 μatm y^{-1} in the Antarctic Ocean. At stationary sites in the western subarctic North Pacific (47°N, 160°E and 44°N, 155°E) the rate was +2.1 μatm y^{-1} during 1999–2016 (Wakita et al. 2017), and for meridional transects from low to mid-latitudes (3°N–34°N, 137°E) the rate was +0.8 and +1.5 μatm y^{-1} during the periods 1984–1997 and 1999–2009, respectively (Midorikawa et al. 2012). Even when restricted to the near-shore side north of the Kuroshio current (31°N–34°N, 137°E), the rate was +1.5 μatm y^{-1} during 1994–2008 (Ishii et al. 2011). Although there were some regional differences in pCO_2^{sea} increase rates for open waters, they have been considered comparable to the increase rate of atmospheric pCO_2, suggesting that air-sea CO_2 exchange was the primary control on surface water CO_2 regulation. In contrast, high increase rates have been reported for inner bay waters in Japan as well as Sagami Bay: +5.8 μatm y^{-1} in Tokyo Bay and +3.2 μatm y^{-1} in Ise Bay (Tokoro et al. 2021). There must be some cause for these remarkably faster increases of bay water pCO_2^{sea} compared to that of pCO_2^{air}, which is discussed below.

Such faster pCO_2^{sea} increasing trends have been found at several coastal stations located

on the northwestern European shelf (3.0–3.5 μatm y^{-1}, Gac et al. 2021) and in the broad southeastern US coastal waters (3.0–3.2 μatm y^{-1} on the middle and outer shelves, 3.2–3.7 μatm y^{-1} in the coastal zone and on inner shelf, Reimer et al. 2017). Gac et al. (2021) suggested that 31–37% of the pCO_2^{sea} trend over the 2008–2020 period in the southern Western English Channel was caused by the effect of SST rise due to global warming (4.23% increase in pCO_2^{sea} per °C, Takahashi et al. 1993). Reimer et al. (2017) also attributed the 26-year trend of pCO_2^{sea} increasing on the middle to outer shelf partly to increased SST, while it in the inner zone was due to the laterally advected high pCO_2^{sea} and organic matter-rich waters from land. However, such a thermal effect did not contribute to the pCO_2^{sea} increasing trend in Sagami Bay because no significant trend is found in our SST dataset (2001–2009) at S3. Rather, the bay-wide average annual SST from another source (Tokyo Regional Headquarters, JMA; https://www.data.jma.go.jp/tokyo/shosai/umi/kaiyou/sst/index.html, in Japanese) shows a significant downward trend (–0.10 ± 0.02 °C y^{-1}) over the same period. This is not a trend unique to Sagami Bay, but rather a decadal variability with a maximum in 2000 and a minimum in 2010 observed over a wide area around Japan (including the East China Sea and the Sea of Japan as well as the western North Pacific off the south coast of Honshu with Kuroshio), which was influenced by variations in the East Asian winter monsoon (Yoshita et al. 2020). In any case, faster increase rate of Sagami Bay pCO_2^{sea} should be caused by local non-thermal processes.

Long-term changing trends were also apparent in other parameters for trapped particles (where deseasonalized monthly means were used, Table 2): POC flux showed a decreasing trend of −2.2 mg m^{-2} d^{-1} (y^{-1}) and PN-$\delta^{15}N$ an increasing trend of +0.2‰ y^{-1} (p <0.001, Fig. 2c). The interannual increase in PN-$\delta^{15}N$ implies a decrease in nitrogenous

nutrient availability (e.g., Sukigara and Saino 2006; Mino et al. 2020), which may have reduced primary productivity and led to a downward trend in POC exports to depth. Notably, the magnitude of this decreasing trend in POC flux is comparable to the decrease in the Bay CO_2 uptake by 1.7 mg m^{-2} d^{-1} per year presumed from the rate of change of CO_2 flux relative to ΔpCO_2 (0.89 mg m^{-2} d^{-1} (μatm^{-1}), Fig. 7) and the ΔpCO_2 increasing trend (+1.9 μatm y^{-1}). This may imply a link between the two (the supposed "biological pump"), although the POC export can only account for approximately 60% of the CO_2 uptake.

Significant pCO_2^{sea} increase rate in each season was found except in autumn, with a particularly large increase rate of +4.9 μatm y^{-1} for summer pCO_2^{sea} (p <0.001, Table 2). This increase, along with the effect of reduced wind speed, caused a large, statistically significant decrease (p = 0.0211) in CO_2 uptake at a rate of +4.1 mg m^{-2} d^{-1} (y^{-1}). There was no significant long-term trend in POC flux, however, a decreasing trend in summer organic carbon concentration (OC%, –0.52% y^{-1}, p = 0.0131) of trapped particles may also indicate reduced organic matter production. Although not detectable during the summer, the upward trend in PN-$\delta^{15}N$ in both spring and autumn that suggests long-term nutrient depletion in the stratified upper waters, and the resulting reduced organic matter

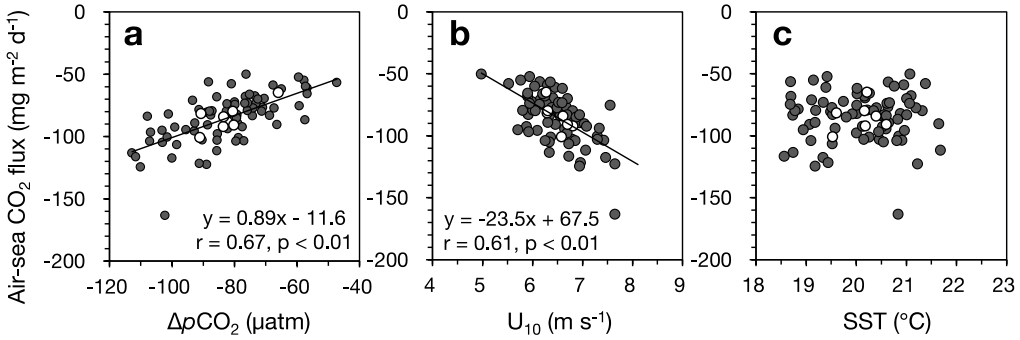

Fig. 7 Scatter plots between deseasonalized monthly means: air-sea CO_2 flux versus (a) ΔpCO_2, (b) U_{10}, and (c) SST. Open circles indicate annual means in 2001–2008 (except 2006). The solid line in panels a and b indicates a linear regression.

production was likely driving the high summer pCO_2^{sea} increase. This is also supported by the summer POC:CO_2 flux ratio of 1.07, which is highest among seasons, implying a more direct link between both carbon fluxes.

The question remains regarding the reason for reduced nutrient availability. It should be noted that nutrient data from monthly cruise observations between January 2000 and October 2007 did not show a clear downward trend in summer concentrations. This discrepancy with our speculation should be addressed in further studies, perhaps using available data not only from S3 but from other sites in the Bay to determine whether our proposed decreasing trend in nutrient availability and increasing pCO_2^{sea} is a Bay-wide or localized occurrence. This is because, as seen in Fig. 4, there was a non-uniform pCO_2^{sea} distribution in the stratified surface water during July and September, unlike during November with well-mixed column. As these are greatly influenced by the Kuroshio warm water intrusion and the associated changes in the current field in the Bay, the type of water mass distribution in the surface layer in summer may determine the CO_2 uptake ability of the central part or the Bay as a whole. As described above, Kuroshio warm water intrusion is sensitive to changes in the Kuroshio path, and therefore, it would not be surprising if a long-term trend in the frequency of inflow of Kuroshio water (likely with high pCO_2^{sea} and less nutrients) was found. If the contribution of Kuroshio warm water to the upper layer of the bay were to increase, there should be an upward trend in SST at S3, but this may be offset by the above-mentioned decadal SST decrease of waters around Japan, including Kuroshio warm water, during the period. For these analyses, the Bay-wide surface-current field based on high-frequency oceanic radar data would be useful.

5 Conclusions

Sediment trap experiments conducted at 150 m during 2001–2009 in Sagami Bay provide time series data on POC settling flux and its $\delta^{13}C$ that were little modified heterotrophically. We applied the empirical inverse relationship between surface suspended POC-$\delta^{13}C$ and [CO_2] derived from multiple cruise observations to trapped POC-$\delta^{13}C$ and successfully reconstructed a weekly time series of pCO_2^{sea} with 28 μatm accuracy over 8.5 years. Using time series of ΔpCO_2, k_{CO2} and K_0, the air-sea CO_2 fluxes were also calculated, and their seasonal and long-term changes were discussed.

The estimated pCO_2^{sea} in the Bay varied by 190 μatm with a mean of 296 μatm, showing an annual cycle with minimum and maximum values in spring and autumn, respectively. Except for a few data points, pCO_2^{sea} was always below the pCO_2^{air} level, resulting in an oceanic CO_2 uptake flux with a mean of 82 mg m^{-2} d^{-1}. This CO_2 flux is very large on a global scale, suggesting that Sagami Bay is an efficient sink for atmospheric CO_2. In contrast, the mean vertical POC export flux was 50 mg m^{-2} d^{-1}, accounting for only 60% of the CO_2 uptake. Although there is 29% uncertainty in the estimated CO_2 flux, it is possible that some of the absorbed CO_2 was removed horizontally from the Bay via surface water exchange (e.g., associated with the Kuroshio warm water intrusion). If true, this process should be studied in more detail for evaluations of future coastal CO_2 sequestration capacity.

CO_2 uptake in winter and spring is approximately twice that in summer and autumn, primarily owing to low pCO_2^{sea} in winter and spring, accompanied by larger gas exchange coefficients from higher wind speeds. This seasonal variation in pCO_2^{sea} can be explained by the effects of temperature change via gas solubility and the effect of DIC change. In general, DIC changes depending on winter enrichment due to vertical mixing and

biological consumption from spring onward. Following the method of Takahashi et al. (2002), the effects of temperature and DIC changes were separated. The calculated temperature effect on pCO_2^{sea} of 155 μatm was slightly larger than the DIC effect of 144 μatm. However, the impact of DIC change was large on a global scale, implying a strong pCO_2^{sea} regulating function of active biological activity in coastal environments.

Long-term trends in parameters were examined using time series of deseasonalized anomalies. During the observation period, there was no significant trend in CO_2 uptake in the Bay, however, the ΔpCO_2 tended to be higher (i.e., pCO_2^{air} and pCO_2^{sea} converged) by 1.9 μatm each year. This was primarily due to the pCO_2^{sea} having a increase rate of +3.9 μatm y^{-1}, approximately twice that of pCO_2^{air}. This large increase rate of pCO_2^{sea} was accompanied by a concurrent decreasing trend in POC flux of −2.2 mg m^{-2} d^{-1} (y^{-1}) and an increasing trend in PN-$\delta^{15}N$ of +0.2‰ y^{-1}. Significant pCO_2^{sea} increase rates were found except in autumn. In particular, a remarkably high increase rate of +4.9 μatm y^{-1} was found in summer, with a decrease in CO_2 uptake by 4.1 mg m^{-2} d^{-1} (y^{-1}) over time. In summer with a high POC:CO_2 flux ratio of > 1, the long-term decrease in nutrient availability and the consequent reduction in organic matter production are likely driving the high pCO_2^{sea} increase rate. However, we should consider whether this long-term trend in the upper layer is a Bay-wide or local occurrence, taking into account the current field and water mass distribution in the Bay. Regardless, it is necessary to monitor the pCO_2^{sea} in Sagami Bay to assess whether its faster increase over pCO_2^{air} as revealed in this study, will continue in the future and reduce CO_2 absorption in the long term. From the perspective of data comparison, if possible, this should be conducted by a method based on sediment trap experiments and stable isotope measurements, as in this study.

Acknowledgments

We thank the Captain and crew of the T/V Seiyo-maru, and scientists and students of TUMSAT, for their help with moored sediment trap deployments. We are also grateful to the officers and crew of the R/V Tansei-maru and JAMSTEC for their support during the cruises and to Takuji Hosaka, TUMSAT, for his management of the Tansei-maru cruise data. We also thank Daisuke Takahashi, Tokai University, Japan, for his assistance with analyzing the Oshima weather station wind speed data and NGSST data, and we thank Tetsuya Nakamura, NiGK, for his technical support with the sediment trap mooring. Data preparation from monthly observation cruises on the Seiyo-maru was supported by the Sumitomo Foundation. The Core Research for Evaluation of Science and Technology (CREST), and the Solution Oriented Research for Science and Technology (SORST) programs, the Japan Science and Technology Agency, supported a large part of this study, and we thank Toshiro Saino, the principal investigator of these programs, for his leadership. Finally, we also express our deep thanks to the editor and anonymous reviewers who provided many helpful and constructive comments.

Author contributions: YM contributed to the study conception and design. Field observations, chemical measurements were performed by CS, AW, AM, KU-M and TI, data analysis by YM and MW. The first draft of the manuscript was written by YM and all authors commented on previous versions of the manuscript. All authors read and approved the final manuscript.

Data availability: The datasets generated and/or analyzed during the current study are available from the corresponding author on reasonable request.

Declarations

Conflict of Interests: The authors declare no competing financial interests.

References

Aita MN, Tadokoro K, Ogawa NO, Hyodo F, Ishii R, Smith SL, Saino T, Kishi MJ, Saitoh SI, Wada E (2011) Linear relationship between carbon and nitrogen isotope ratios along simple food chains in marine environments. J. Plankton Res 33:1629–1642. doi:10.1093/plankt/fbr070

Bakker DCE, Alin SR, Castaño-Primo R, Cronin M, Gkritzalis T, et al. (2016) A multi-decade record of high-quality fCO_2 data in version 3 of the Surface Ocean CO_2 Atlas (SOCAT). Earth Syst. Sci. Data 8:383–413. doi:10.5194/essd-8-383-2016

Bentaleb I, Fontugne M (1998) The role of the Southern Indian Ocean in the glacial to interglacial atmospheric CO_2 change: organic carbon isotope evidence. Global Planet Change 16–17:25–36. doi:10.1016/S0921-8181(98)00004-6

Bentaleb I, Fontugne M, Descolas-Gros C, Girardin C, Mariotti A, Pierre C, Brunet C, Poisson A (1998) Carbon isotopic fractionation by phytoplankton in the Southern Indian Ocean: relationship between $\delta^{13}C$ of particulate organic carbon and dissolved carbon dioxide. J Mar Syst 17:39–58. doi:10.1016/s0924-7963(98)00028-1

Buesseler KO, Steinberg DK, Michaels AF, Johnson RJ, Andrews JE, Valdes JR, Price JF (2000) A comparison of the quantity and quality of material caught in a neutrally buoyant versus surface-tethered sediment trap. Deep-Sea Res I 47:277–294. doi:10.1016/S0967-0637(99)00056-4

Buesseler K, Antia AN, Chen M, Fowler SW, Gardner WD, Gustafsson O, Harada K, Michaels AF, van der Loeff MR, Sarin M, Steinberg DK, Trull T (2007) An assessment of the use of sediment traps for estimating upper ocean particle fluxes. J Mar Res 65: 345–416. doi:10.1357/002224007781567621

Burkhardt S, Amoroso G, Riebesell U, Sultemeyer D (2001) CO_2 and HCO_3^- uptake in marine diatoms acclimated to different CO_2 concentrations. Limnol Oceanogr 46:1378–1391. doi:10.4319/lo.2001.46.6.1378

Chen CTA, Borges AV (2009) Reconciling opposing views on carbon cycling in the coastal ocean: Continental shelves as sinks and near-shore ecosystems as sources of atmospheric CO_2. Deep-Sea Res 56:578–590. doi:10.1016/j.dsr2.2009.01.001

Chen CTA, Huang TH, Chen YC, Bai Y, He X, Kang Y (2013) Air–sea exchanges of CO_2 in the world's coastal seas. Biogeosciences 10:6509–6544. doi:10.5194/bg-10-6509-2013

Conte MH, Ralph N, Ross EH (2001) Seasonal and interannual variability in deep ocean particle fluxes at the Oceanic Flux Program (OFP)/Bermuda Atlantic Time Series (BATS) site in the western Sargasso Sea near Bermuda. Deep-Sea Res II 48:1471–1505. doi:10.1016/S0967-0645(00)00150-8

Dhairs F, Kopczynska E. Nielsen P, Lancelot C, Bakker DCE, Koeve W, Goeyens L (1997) $\delta^{13}C$ of Southern Ocean suspended organic matter during spring and early summer: regional and temporal variability. Deep-Sea Res I 44:129–142. doi:10.1016/S0967-0645(96)00073-2

DeNiro MJ, Epstien S (1978) Influence of diet on the distribution of carbon isotopes in animals. Geochim Cosmochim Acta 42:495–506. doi:10.1016/0016-7037(78)90199-0

Farquhar GD, O'Leary MH, Berry JA (1982) On the relationship between carbon isotope discrimination and the intracellular carbon dioxide concentration in leaves. Aust J Plant Physiol 9:121–137. doi:10.1071/PP9820121

Fischer G, Muller PJ, Wefer G (1998) Latitudinal $\delta^{13}C_{org}$ variations in sinking matter and

sediments from the South Atlantic: effects of anthropogenic CO_2 and implications for paleo-pCO_2 reconstructions. J Mar Syst 17:471–495. doi:10.1016/S0924-7963(98)00059-1

Fischer G, Romero OE, Karstensen J, Baumann KH, Moradi N, Iversen M, Ruhland G, Klann M, Kortzinger A (2021) Seasonal flux patterns and carbon transport from low-oxygen eddies at the Cape Verde Ocean Observatory: lessons learned from a time series sediment trap study (2009-2016). Biogeosciences 18:6479-6500. doi:10.5194/bg-18-6479-2021

Francois R, Altabet MA, Goericke R, McCorkle DC, Brunet C, Poisson A (1993) Changes in the $\delta^{13}C$ of surface water particulate organic matter across the subtropical convergence in the SE Indian Ocean. Global Biogeochem Cycles 7:627–644. doi:10.1029/93GB01277

François R, Altabet MA, Yu E-F, Sigman DM, Bacon MP, Frank M, Bohrmann G, Bareille G, Labeyrie LD (1997) Contribution of Southern Ocean surface-water stratification to low atmospheric CO_2 concentrations during the last glacial period. Nature 389:929–935. doi:10.1038/40073

Friedlingstein P, Jones MW, O'Sullivan M, Andrew RM, Bakker DCE, Hauck J, Le Quéré C, Peters GP, et al. (2022) Global Carbon Budget 2021. Earth System Science Data 14:1917–2005. doi:10.5194/essd-14-1917-2022

Fry B (1988) Food web structure on Georges Bank from stable C, N, and S isotopic compositions. Limnol Oceanogr 33:1182–1190. doi:10.4319/lo.1988.33.5.1182

Fujiki T, Hosaka T, Kimoto H, Ishimaru T, Saino T (2008) In situ observation of phytoplankton productivity by an underwater profiling buoy system: Use of fast repetition rate fluorometry. Mar Ecol Prog Ser 353:81–88. doi:10.

3354/meps07151

Gac J-P, Marrec P, Cariou T, Grosstefan E, Macé É, Rimmelin-Maury P, et al. (2021) Decadal dynamics of the CO_2 system and associated ocean acidification in coastal ecosystems of the north east Atlantic Ocean. Front. Mar. Sci. 8:688008. doi:10.3389/fmars.2021.688008

Grasshoff K, Ehrhardt M, Kremling K (1999) Methods of Seawater Analysis, 3rd edn. WILEY-VCH Verlag GmbH, Weinheim.

Hashihama F, Horimoto N, Kanda J, Furuya K, Ishimaru T, Saino T (2008) Temporal variation in phytoplankton composition related to water mass properties in the central part of Sagami Bay. J Oceanogr 64:23–37. doi:10.1007/s10872-008-0002-8

Hashimoto S, Horimoto N, Yamaguchi Y, Ishimaru T, Saino T (2005) Relationship between net and gross primary production in the Sagami Bay, Japan. Limnol Oceanogr 50:1830–1835. doi:10.4319/lo.2005.50.6.1830

Hinata H, Miyano M, Yanagi T, Ishimaru T, Kasuya T, Kawamura H (2003) Short-period fluctuations of surface circulation in Sagami Bay induced the Kuroshio warm water intrusion through Oshima west channel. Oceanography in Japan 12:167–184. doi:10.5928/kaiyou.12.167 (in Japanese with an English abstract)

Honda MC, Kawakami H, Matsumoto K, Wakita M, Fujiki T, Mino Y, Sukigara C, Kobari T, Uchimiya M, Kaneko R, Saino T (2015) Comparison of sinking particles in the upper 200 m between subarctic station K2 and subtropical station S1 based on drifting sediment trap experiments. J Oceanogr 72:373–386. doi:10.1007/ s10872-015-0280-x

Ishii M, Kosugi N, Sasano D, Saito S, Midorikawa T, Inoue HY (2011) Ocean

acidification off the south coast of Japan: A result from time series observations of CO_2 parameters from 1994 to 2008. J Geophys Res 116:C06022. doi:10.1029/2010JC006831

Jasper JP, Hayes JM (1990) A carbon isotope record of CO_2 levels during the late quaternary. Nature 347:462–464. doi:10.1038/347462a0

Kayanne H, Hata H, Kudo S, Yamano H, Watanabe A, Ikeda Y, Nozaki K, Kato K, Negishi A, Saito H (2005) Seasonal and bleaching-induced changes in coral reef metabolism and CO_2 flux. Global Biogeochem Cycles 19:GB3015. doi:10.1029/2004GB002400

Keeling CD, Brix H, Gruber N (2004) Seasonal and long-term dynamics of the upper ocean carbon cycle at Station ALOHA near Hawaii. Global Biogeochem Cycles 18:GB4006. doi:10.1029/2004GB002245

Keller K, Morel FMM (1999) A model of carbon isotopic fractionation and active carbon uptake in phytoplankton. Mar Ecol Prog Ser 182: 295–298. doi:10.3354/meps182295

Kennedy H, Robertson J (1995) Variations in the isotopic composition of particulate organic carbon in surface waters along an 88°W transect from 67°S to 54°S. Deep-Sea Res II 42:1109–1122. doi:10.1016/0967-0645(95)00069-3

Knauer GA, Martin JH, Bruland KW (1979) Fluxes of particulate carbon, nitrogen, and phosphorous in the upper water column of the northeast Pacific. Deep-Sea Res 26:97–108. doi:10.1016/0198-0149(79)90089-X

Kubo A, Maeda Y, Kanda J (2017) A significant net sink for CO_2 in Tokyo Bay. Sci Rep 7:44355. doi:10.1038/srep44355

Laws EA, Popp BN, Bidigare RR, Kennicutt MC, Macko SA (1995) Dependance of

phytoplankton carbon isotopic composition on growth rate and $[CO_2]_{aq}$: theoretical considerations and experimental results. Geochim Cosmochim Acta 59:1131–1138. doi:10.1016/0016-7037(95)00030-4

Laws EA, Popp BN, Cassar N, Tanimoto J (2002) ^{13}C discrimination patterns in oceanic phytoplankton: likely influence of CO_2 concentrating mechanisms, and implications for palaeoreconstructions. Funct Plant Biol 29:323–333. doi:10.1071/PP01183

Lourey MJ, Trull TW, Tilbrook B, (2004) Sensitivity of $\delta^{13}C$ of Southern Ocean suspended and sinking organic matter to temperature, nutrient utilization, and atmospheric CO_2. Deep-Sea Res I 51:281–305. doi:10.1016/j.dsr.2003.10.002

Masuzawa T, Li T, Duan Y, Yamamoto M, Hibi Y, Nakatsuka T, Kitazato H, Kato Y, (2003) Temporal variation in mass fluxes and the major components of sinking particles in Sagami Bay, off Japan. Prog Oceanogr 57:59–75. doi:10.1016/S0079-6611(03)00051-X

Midorikawa T, Ishii M, Kosugi N, Sasano D, Nakano T, Saito S, Sakamoto N, Nakano H, Inoue HY (2012) Recent deceleration of oceanic pCO_2 increase in the western North Pacific in winter. Geophys Res Lett 39:L12601. doi:10.1029/2012GL051665

Mino Y, Sukigara C, Kawakami H, Honda MC, Matsumoto K, Wakita M, Kitamura M, Fujiki T, Sasaoka K, Abe O, Kaiser J, Saino T (2016) Seasonal variations in the nitrogen isotopic composition of settling particles at station K2 in the western subarctic North Pacific. J Oceanogr 72:819–836. doi:10.1007/s10872-016-0381-1

Mino Y, Sukigara C, Honda MC, Kawakami H, Wakita M, Sasaoka K, Yoshikawa C, Abe

O, Kaiser J, Kimoto K, Kitamura M, Fujiki T, Matsumoto K, Saino T (2020) Seasonal and interannual variations in nitrogen availability and particle export in the northwestern North Pacific subtropical gyre. J Geophys Res Oceans 125:e2019JC015600. doi:10.1029/2019JC015600

Mitbavkar S, Saino T, Horimoto N, Kanda J, Ishimaru T (2009) Role of Environment and Hydrography in Determining the Picoplankton Community Structure of Sagami Bay, Japan. J Oceanogr 65:195–208. doi:10.1007/s10872-009-0019-7

Miyake Y, Wada E (1967) The abundance ratio of $^{15}N/^{14}N$ in marine environments. Rec Oceanogr Works Jpn 9:37–53.

Muller-Karger FE, Varela R, Thunell R, Luerssen R, Hu CM, Walsh JJ (2005) The importance of continental margins in the global carbon cycle. Geophys Res Lett 32:L01602. doi.org/10.1029/2004GL021346

O'Leary MH (1981) Carbon-isotope fractionation in plants. Phytochemistry 20:553–567. doi:10.1016/0031-9422(81)85134-5

Popp BN, Laws EA, Bidigare RR, Dore JE, Hanson KL, Wakeham SG (1998) Effect of phytoplankton cell geometry on carbon isotopic fractionation. Geochim Cosmochim Acta 62:69–77. doi:10.1016/S0016-7037(97)00333-5

Rau GH, Takahashi T, Des Marias DJ (1989) Latitudinal variations in plankton $\delta^{13}C$: Implications for CO_2 and productivity in past oceans. Nature 341:516–518. doi:10.1038/341516a0

Rau GH, Froelich PN, Takahashi T, Des Marias DJ (1991a) Does sedimentary organic 6°C record variations in quaternary ocean [CO_2(aq)]. Paleoceanography 6:335–347. doi:10.1029/91PA00321

Rau GH, Takahashi T, Des Marais DJ, Sullivan CW (1991b) Particulate organic matter

$\delta^{13}C$ variations across the Drake Passage. J Geophys Res 96:15131–15135. doi:10.1029/91JC01253

Rau GH, Takahashi T, Des Marias DJ, Repeta DJ, Martin JH (1992) The relationship between $\delta^{13}C$ of organic matter and [CO_2(aq)] in ocean surface water. Data from a JGOFS site in the Northeast Atlantic Ocean and a model. Geochim Cosmochim Acta 56:1413–1417. doi:10.1016/0016-7037(92)90073-R

Rau GH (1994) Variations in sedimentary organic $\delta^{13}C$ as a proxy for past changes in ocean and atmospheric CO_2 concentrations. In: Zahn R et al (eds) Carbon cycling in the Glacial Ocean: Constrains on the ocean's role in global change. NATO ASI Series, vol 17. Springer, Heidelberg, pp 307–321. doi:10.1007/978-3-642-78737-9_13

Raven JA (1997) Inorganic carbon acquisition by marine autotrophs. Adv Bot Res 27:85–209. doi:10.1016/S0065-2296(08)60281-5

Reimer JJ, Wang H, Vargas R, Cai W-J (2017) Multidecadal fCO_2 increase along the United States southeast coastal margin. J Geophys Res Oceans 122:10,061–10,072. doi:10 1002/2017JC013170

Roobaert A, Laruelle GG, Landschutzer P, Gruber N, Chou L, Regnier P (2019) The spatiotemporal dynamics of the sources and sinks of CO_2 in the global coastal ocean. Global Biogeochem Cycles 33:1693–1714 doi:10.1029/2019GB006239

Sabine CL, Feely RA, Gruber N, Key RM, Lee K, Bullister JL, Wanninkhof R, Wong CS, Wallace DWR, Tilbrook B, Millero FJ, Peng TH, Kozyr A, Ono T, Rios AF (2004) The oceanic sink for Anthropogenic CO_2. Science 305:367–371. doi:10.1126/science.1097403

Saino T (2007) Ocean primary productivity monitoring using an underwater profiling

buoy system. Bulletin on Coastal Oceanography 45: 17–28. doi:10.32142/engankaiyo.45.1_17 (in Japanese with an English abstract)

Sukigara C, Saino T (2005) Temporal variations of $\delta^{13}C$ and $\delta^{15}N$ in organic particles collected by a sediment trap at a time-series station off the Tokyo Bay. Cont Shelf Res 25:1749–1767. doi:10.1016/j.csr.2005.06.002

Sukigara C, Saino T (2006) A 7-year increasing trend of ^{15}N in sinking particles at the mouth of the Tokyo Bay. Geophys Res Lett 33:L09607. doi:10.1029/2006GL025982

Sukigara C, Otosaka S, Horimoto-Miyazaki N, Mino Y (2022) Temporal variation of particulate organic carbon flux at the mouth of Tokyo Bay. J Oceanogr. doi:10.1007/s10872-022-00660-7

Takahashi T, Olafsson J, Goddard JG, Chipman DW, Sutherland SC (1993) Seasonal variation of CO_2 and nutrients in the high-latitude surface oceans: A comparative study. Global Biogeochem Cycles 7:843–878. doi:10.1029/93GB02263

Takahashi T, Sutherland T, Sweeney CS, Poisson C, Metzl N, Tilbrook B, Bates N, Wanninkhof R, Feely RA, Sabine C, Olafsson J, Nojiri Y (2002) Global sea-air CO_2 flux based on climatological surface ocean pCO_2, and seasonal biological and temperature effects. Deep-Sea Res II 49:1601–1622. doi:10.1016/S0967-0645(02)00003-6

Takahashi T, Sutherland SC, Feely RA, Wanninkhof R (2006) Decadal change of the surface water pCO_2 in the North Pacific: A synthesis of 35 years of observations. J Geophys Res Oceans 111:C07S05. doi:10.1029/2005JC003074

Takahashi T, Sutherland SC, Wanninkhof R, Sweeney C, Feely RA, Chipman DW, Hales B, Friederich G, Chavez F, Sabine C, Watson A, Bakker DCE, Schuster U, Metzl

N, Inoue HY, Ishii M, Midorikawa T, Noriji Y, Körtzinger A, Steinhoff T, Hoppema M, Olafsson J, Arnarson TS, Tilbrook B, Johannessen T, Olsen A, Belleby R, Wong CS, Delille B, Bates NR, deBaar HJW (2009) Climatological mean and decadal change in surface ocean pCO_2, and net sea–air CO_2 flux over the global oceans. Deep-Sea Res II 56:554–577. doi:10.1016/j.dsr2.2008.12.009

Tokoro T, Nakaoka S, Takao S, Kuwae T, Kubo A, Endo T, Nojiri Y (2021) Contribution of biological effects to carbonate-system variations and the air–water CO_2 flux in urbanized bays in Japan. J Geophys Res Oceans 126:e2020JC016974. doi:10.1029/2020JC016974

Wakita M, Nagano A, Fujiki T, Watanabe S (2017) Slow acidification of the winter mixed layer in the subarctic western North Pacific. J Geophys Res Oceans 122:6923–6935. doi:10.1002/2017JC013002

Wakita M, Sasaki K, Nagano A, Abe H, Tanaka T, Nagano K, Sugie K, Kaneko H, Kimoto K, Okunishi T, Takada M, Yoshino J, Watanabe S (2021) Rapid reduction of pH and CaCO3 saturation state in the Tsugaru Strait by the intensified Tsugaru Warm Current during 2012–2019. Geophys Res Lett 48: e2020GL091332. doi:10.1029/2020GL091332

Walsh JJ, Carder KL, Muller-Karger FE (1992) Meridional Fluxes of Dissolved Organic Matter in the North Atlantic Ocean. J Geophys Res 97(C10):15625–15637. doi:10.1029/92JC01177

Wanninkhof R (2014) Relationship between wind speed and gas exchange over the ocean revisited. Limnol Oceanogr: Methods 12: 351–362. doi:10.4319/lom.2014.12.351

Waples DW, Sloan JR (1980) Carbon and nitrogen diagenesis in deep sea sediments. Geochim Cosmochim Acta 44:1463–1470. doi:10.1016/0016-7037(80)90111-8

Watanabe A, Kayanne H, Nozaki K, Kato K, Negishi A, Kudo S, Kimoto H, Tsuda M, Dickson AG (2004) A rapid, precise potentiometric determination of total alkalinity in seawater by a newly developed flow-through analyzer designed for coastal regions. Mar Chem 85:75–87. doi:10.1016/j.marchem.2003.09.004

Weiss RF (1974) Carbon dioxide in water and seawater: the solubility of a non-ideal gas. Marine Chem 2:203–215. doi:10.1016/0304-4203(80)90024-9

Yoshita K, Kitamura Y, Nakano T (2020) Decadal variability of sea surface temperature around Japan. Oceanography in Japan 29: 19–36. doi:10.5928/kaiyou.29.2_19 (in Japanese with an English abstract)

Table 1 Annual and seasonal means of atmospheric and seawater pCO_2, their difference (ΔpCO_2), air-sea CO_2 flux and underwater POC flux, trapped particle OC% and PN-$\delta^{15}N$, and the surface environment parameters, sea surface temperature (SST) and wind speed (U_{10}).

Mean	pCO_2^{air}	pCO_2^{sea}	ΔpCO_2	Air-sea CO_2 flux	POC flux	POC:CO_2 flux ratio	OC%	PN-$\delta^{15}N$	SST	U_{10}
	μatm	μatm	μatm	mg m^{-2} d^{-1}	mg m^{-2} d^{-1}		%	‰	°C	m s^{-1}
2001–2008	377	293	–84	–85	53	0.62	9.2	5.5	20.2	6.5
2001–2008[a]	376	296	–80	–82	50	0.60	9.1	5.6	20.6	6.5
Winter (DJF)[a]	380	295	–86	−102	34	0.33	7.3	4.3	17.0	7.2
Spring (MAM)[a]	381	273	–108	−121	49	0.40	9.3	4.6	17.5	6.7
Summer (JJA)[a]	373	297	–76	−58	62	1.07	11.2	6.4	23.0	5.7
Autumn (SON)[a]	374	316	–57	−56	50	0.90	7.9	6.1	22.9	6.4

[a] Means were calculated when all data from 2006 and the end of 2007 were excluded.

Table 2 The rate of change of deseasonalized monthly parameter means during the entire period (2001–2008) and in each season. Only the rate is presented when the trend is significant.

Rate	pCO_2^{air}	pCO_2^{sea}	ΔpCO_2	Air-sea CO_2 flux	POC flux	OC%	PN-$\delta^{15}N$	SST	U_{10}
y^{-1}	μatm	μatm	μatm	mg m^{-2} d^{-1}	mg m^{-2} d^{-1}	%	‰	°C	m s^{-1}
2001-2008[a]	2.0 ± 0.1	3.9 ± 0.7	1.9 ± 0.7		-2.2 ± 0.8		0.2 ± 0.0		
Winter (DJF)[a]	1.9 ± 0.1	3.7 ± 1.6							
Spring (MAM)[a]	2.3 ± 0.1	4.3 ± 1.1			-5.4 ± 1.3		0.3 ± 0.1		
Summer (JJA)[a]	1.8 ± 0.3	4.9 ± 1.0	3.1 ± 1.0	4.1 ± 1.6		−0.52 ± 0.2			−0.15 ± 0.1
Autumn (SON)[a]	2.1 ± 0.2						0.2 ± 0.1		

[a] Rates were calculated when all data from 2006 and the end of 2007 were excluded.

Figure captions:

Fig. 1 (**a**) Location of the study area, (**b**) an enlarged view of the study site in Sagami Bay showing the 100, 200, 500, 1000, 1500, 2000 m isobaths. The star indicates the location of the sediment trap mooring S3 whereas the dot indicates the sampling station in the Bay. The open triangle on Oshima Island indicates the Japan Meteorological Agency weather station. In panel (a) three typical paths of the Kuroshio current are shown: A. typical large meander, B. nearshore nonlarge meander, and C. offshore nonlarge meander.

Fig. 2 Time series data of (**a**) particulate organic carbon (POC) flux (bar), (**b**), particulate organic carbon isotope delta (POC-$\delta^{13}C$, closed circle) and (**c**) particulate nitrogen isotope delta (PN-$\delta^{15}N$, open circle) of trapped particles at 150 m in central Sagami Bay during 2001–2009. Thick line in panel (**a**) indicates 6-week moving average of POC flux after excluding the top 5% high fluxes. Dashed lines in panels indicate statistically significant regressions of deseasonalized monthly means ($p < 0.05$). Note that these regressions were obtained after excluding all data from 2006 and the end of 2007, when extreme values of POC-$\delta^{13}C$ were found (see text).

Fig. 3 Relationship between suspended POC-$\delta^{13}C$ and aqueous CO_2 concentration ($[CO_{2aq}]$) in surface waters collected during 2007 to 2008 in Sagami Bay. Closed and open circles indicate data from station S3 and others.

Fig. 4 Distribution of surface water pCO_2 (pCO_2^{sea}) and suspended POC-$\delta^{13}C$ in Sagami Bay in (**a, e**) July 2007, (**b, f**) November 2007, (**c, g**) July 2008, and (**d, h**) September 2008. Note that pCO_2^{sea} data in 2007 were obtained by an underway measuring system on board while those in 2008 were calculated from both measurements of dissolved inorganic carbon and total alkalinity of surface water samples.

Fig. 5 Time series data of (**a**) pCO_2^{sea} (circle) and atmospheric pCO_2 (pCO_2^{air}, solid line),

(**b**) air-sea CO_2 flux (bar) in the central part of Sagami Bay during 2001 to 2009. For CO_2 flux, negative values indicate oceanic CO_2 uptake. Open circles in panel (**a**) indicate pCO_2^{sea} calculated from "extreme POC-$\delta^{13}C$ values" (see text). CO_2 fluxes associated with these extreme $\delta^{13}C$ are presented as gray bars in panel (**b**). Dashed lines in panel **a** indicate statistically significant regressions of deseasonalized monthly means ($p < 0.05$). Note that these regressions were obtained after excluding all data from 2006 and the end of 2007, when extreme values of POC-$\delta^{13}C$ were found.

Fig. 6 Annual composite time series of (**a**) seawater pCO_2^{sea} (circle), atmospheric pCO_2^{air} (dot), and sea surface temperature (SST, cross), (**b**) pCO_2^{sea} values normalized to the mean annual temperature of 20.1 °C (isothermal pCO_2^{sea}; closed circle) and the mean annual pCO_2^{sea} values corrected for temperature changes (isochemical pCO_2^{sea}; open circle), and (**c**) trapped PN-$\delta^{15}N$ and dissolved inorganic nitrogen (DIN) concentration in the surface waters at S3. The pCO_2^{sea} and pCO_2^{air}, SST and trapped PN-$\delta^{15}N$ were obtained during 2001 to 2009, while DIN concentrations were observed during 2001 to 2007. Note that the linearly de-trended pCO_2^{sea} values for the long-term change are presented in panel **a** and were used to calculate both isochemical pCO_2^{sea} and isothermal pCO_2^{sea} in panel **b** (see text). The PN-$\delta^{15}N$ in panel **c** was also de-trended.

Fig. 7 Scatter plots between deseasonalized monthly means: air-sea CO_2 flux versus (**a**) ΔpCO_2, (**b**) U_{10}, and (**c**) SST. Open circles indicate annual means in 2001–2008 (except 2006). The solid line in panels **a** and **b** indicates a linear regression.

Online Resource 1, 3

"Rapid increase of surface water pCO_2 revealed by settling particulate organic matter carbon isotope time series during 2001–2009 in Sagami Bay, Japan"
submitted to ***Journal of Oceanography***

Yoshihisa Mino, Chiho Sukigara, Atsushi Watanabe, Akihiko Morimoto, Kaori Uchiyama-Matsumoto, Masahide Wakita, and Takashi Ishimaru

Corresponding author:
Yoshihisa Mino (kuro@hyarc.nagoya-u.ac.jp)
Institute for Space-Earth Environment Research, Nagoya University, Nagoya, Japan

Online Resource 1

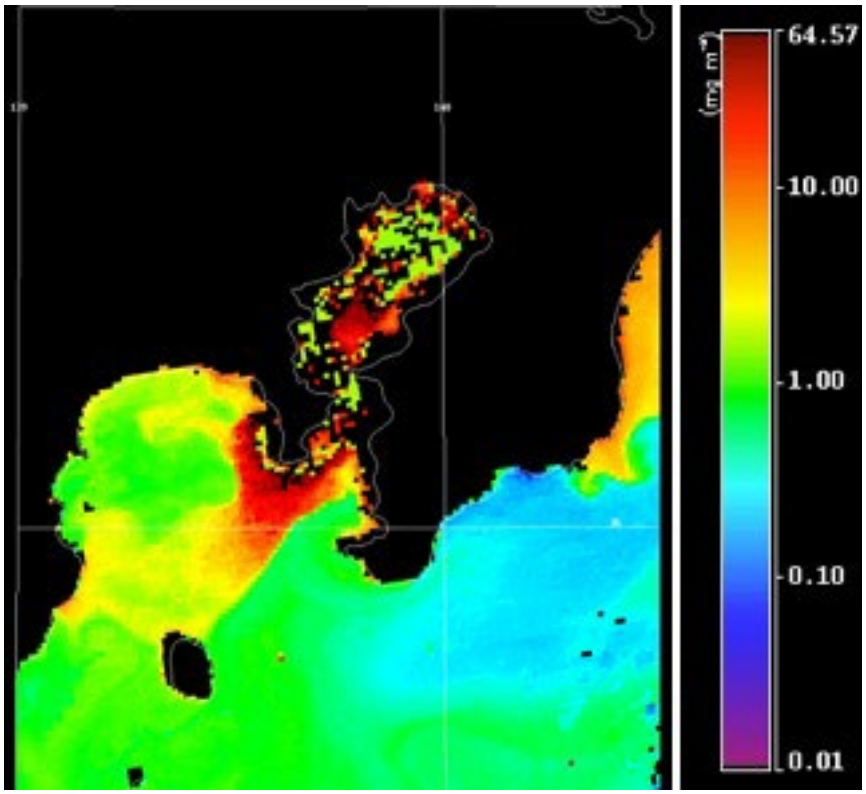

Fig. SI-1 Aqua MODIS 9km, 8-day satellite chlorophyll (Chl) *a* image at the study region for 16–23 October 2006, showing that surface Chl *a* with high concentration spreads from within Tokyo Bay to central Sagami Bay.

Online Resource 3

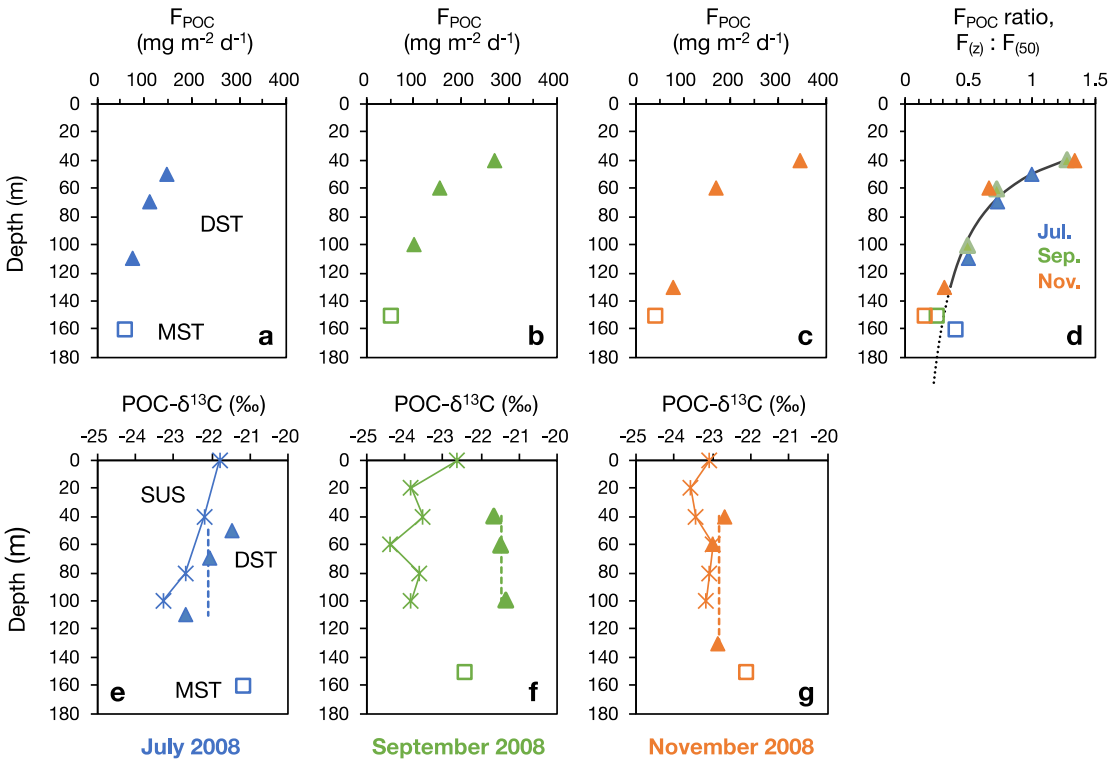

Fig. SI-3 Results of multi-layer, surface tethered drifting sediment trap (DST) experiments in July, September, and November 2008 at station S3. Profiles of (**a-c**) POC flux, F_{POC}, (**d**) flux ratio against the flux at 50 m, $F_{(z)}$:$F_{(50)}$, (**e-g**) particulate organic carbon isotope delta, POC-$\delta^{13}C$. Closed triangle and open square in all panels indicates DST particle and moored sediment trap (MST) particle, respectively. Asterisk in panels (**e-g**) indicates suspended particle. Solid line in panel (**d**) indicates the regression of POC flux vertical attenuation derived by fitting the Martin curve to the all DST-F_{POC} dataset: $F_{(z)}/F_{(50)} = (z/50)^{-1.08}$. Note that the estimated flux ratio at 150–160 m from this regression was consistent well with the MST data. Vertical dashed line in panels (**e-g**) indicates mean POC-$\delta^{13}C$ of DST particles.